Comparison of the Results Inferred from OMA and IEMA

Kemal Beyen,
Kocaeli University, Kocaeli, Turkey, kbeyen@kocaeli.edu.tr

Mustafa Kutanis
Sakarya University, Sakarya, Turkey, mkutanis@gmail.com.tr

ABSTRACT: Experimental modal analysis (EMA) identifies a modal model from recorded test inputs and measured vibration responses. Recently, system identification techniques were developed to identify the modal model for operational responses with output-only model (OMA). OMA takes advantage of the ambient excitations. During EMA, scaled structure reconstructed to test in laboratory conditions can differ significantly from the real-life operating conditions. Insitue experimental modal analysis (IEMA), which is alternative to EMA intrudes more accurate and consistent results along with robust techniques.

In this study, assessment of the input noise, power of the input and influence to results is studied using real test data recorded from insitue experiments. In case of harmonic excitations in the output only model, story transfer functions are proposed to eliminate the effects of the pseudo-modes assuming that all structural members as well as the rigid diaphragm floors in the structure will be exposed to identical harmonic input.

1 INTRODUCTION

Operational modal analysis (OMA) allows us to extract the modal properties of structures based on their response to non-measured stationary white noise, accepting that the structure responses to operational excitations (i.e., ambient). In this study, particularly under unknown harmonic excitations in addition to noise, output-only approach is utilized to extract the modal parameters such as Eigen frequencies and corresponding modal damping and displacements for a reinforced concrete bare frame structure using observer-Kalman-identification with Eigen realization algorithm (OKID-ERA). OKID-ERA is used to estimate the poles of the system (i.e., state space model) for the transfer functions (i.e., frequency response functions) between structural responses at the specific observation points and the white Gaussian noise input. Results obtained for ambient and forced vibration response recordings are compared and discussed for real test structure under real field conditions. Accuracy and consistency of the output only approach for an insitue experiment is evaluated for the operational responses of the cases. Gaussian white noise, which is used for the non-measured input force, is also studied to point out the questionable effects.

In the presence of additional large amplitude harmonic excitation, although OMA procedures are still applicable, the harmonic response components can be identified as pseudo-modes of the system with some values of damping ratio. However, as expected, theoretically zero damping for the pseudo-modes should have been characteristic property under harmonic forced vibrations. Such fake peaks make difficult to distinguish true Eigen responses (i.e., modal peaks) from harmonic response. Filtering the operational response history might be a solution to remove such harmonic effects, if characteristics of the input are known a priori. However, it is known that filtering also removes part of the structural response. On the other hand, in case of the close frequencies, (i.e., frequency of the harmonic input motion equal/around the Eigen-frequency) Eigen analysis is especially exposed to incorrect (due to rapidly building new stiffness states against acting forces) or concealed (filtered) response of the system.

In this study, assessment of input noise, power of the input and influence to results is studied using real test data recorded from insitue experiments. In case of harmonic excitations in the output only model, story transfer functions are proposed to remove the effects of the pseudo-modes assuming that all structural members as well as the rigid diaphragm floors in the structure will be exposed to identical harmonic input. Both nonparametric (i.e., spectral) and parametric techniques are employed in order to cross-validate the results of the output only models. Using recorded input and output data sets, characteristic structural transfer functions are estimated only for reference. Along with well known spectral analysis, in parametric analysis, OKID/ERA is adopted and performed in three major computational steps: (1) The observer Markov parameters are calculated with OKID. (2) From the observer Markov parameters, OKID, this time, retrieves the system Markov parameters. (3) ERA is utilized with the system Markov parameters to realize the discrete time state-space (SS) system matrices, *A*, *B*, *C* and *D*. Since OKID has an asymptotically stable observer, it recovers an optimal observer Kalman filter gain as part of the identification process. Details with derivations can be found in Juang (Juang 1985, Juang et al. 1994). Matlab (2002) was used for coding the necessary routines utilized in this study.

2 AMBIENT MEASUREMENT AND INSITUE EXPERIMENTAL TEST

This paper aims to cross check the results obtained from OMA and IEMA in terms of accuracy and physical interpretation. For such a comparative work, a series of measurements were performed on suitable buildings in the Marmara region, where the recent great Turkish earthquakes hit. The case study structure is a 5-storey reinforced concrete (RC) bare frame apartment building that was under construction during the 17 August 1999 Kocaeli earthquake. Minor damages on some columns are inspected. Plan of the structure can be seen in Figure 1. Infill walls were partially worked out in some bays in the ground floor. The regular storey height is 2.80m except at the substory.

In order to record the ambient responses and harmonic responses of the structure, 10 structurally important observation points were instrumented with three component accelerometers as shown in Figure 1. Locations of the sensors are key points believed to reflect the structural characteristics. The equipment used for the measurement and data acquisition are DAC series accelerometers manufactured by Arel electronics (Arel 2010). In case of the force vibration tests, eccentric vibration generator manufactured by Kinemetrics was mounted at the mass center of the top floor as shown in Figure 1.

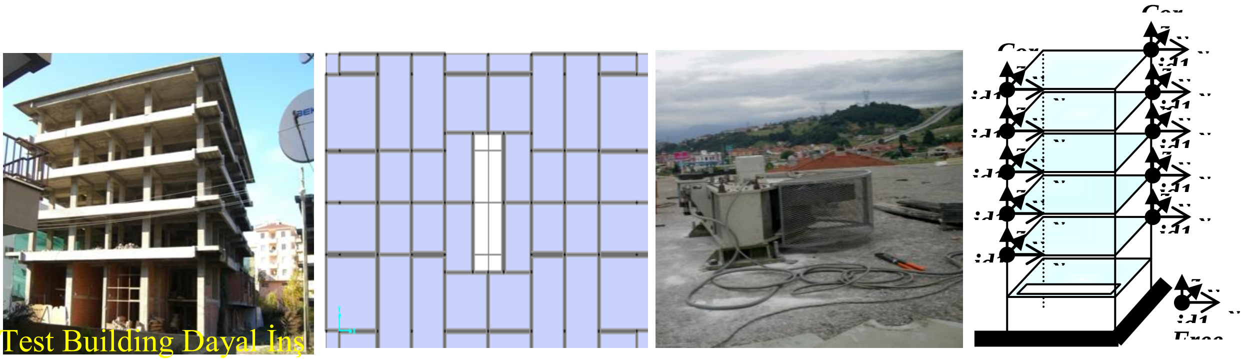

Figure 1 : Test building in Sakarya, plan view, eccentric harmonic vibration generator on the top floor and locations of the instruments in the near left and far right corners in the drawing.

3 DATA PROCESSING AND DISCUSSION

In the all recordings, data were sampled at 200 Hz. In order to quantify and minimize the effects of changing environmental conditions, six sets of ambient vibration measurements were carried out to identify the dynamic characteristics of the structure along with the free-field measurements in the courtyard. In case of ambient vibration measurement, each set was recorded for duration of 5 minutes. In the forced vibration tests, recording time in data acquisition was changing 2 to 6 minutes depending upon structural responses and test conditions. Some basic preprocessing tasks such as base-line correction (linear and, if necessary polynomial), decimation for eliminating high frequency spikes in the record, band filtering between frequencies of 0.2 Hz and the Nyquist frequency of 100 Hz were performed.

As distinguishable examples, ambient and forced vibration of the structural points and the ground data as a free field are plotted for x direction, as shown in Figure 2, after preprocessing the data. Subsequently, the corrected data were Fourier transformed smoothing by SGolay filter (Matworks, 2002) with window length of 5 samples and polynomial degree of 2 for noise reduction without loss of high frequency information component. Figure 3 shows the Fourier amplitude spectra of ambient and forced vibration time histories for the ten structural observation points. In order to identify the characteristic structural behavior in frequencies, transfer functions between the structural sensor points and the base have been calculated and are plotted only for x direction for ambient and forced vibration cases in Figure 4. Observed additional peaks in the lower frequency region may be attributed to the harmonic responses at first glance. Although individual small differences in amplitudes of the transfer functions are seen, general consistency is dominant. In Tables 1 and 2, under forced and ambient vibrations, modal frequencies and corresponding modal damping ratios for identified first 12 modes in x direction are given. In Table 3, modal displacements for identified first 12 modes for ambient and forced vibrations in x direction are tabulated. Modal displacements inferred from ambient and forced vibrations are consistent and depict identically polarized structural mode shapes.

Natural frequencies and modal damping ratios of the modal properties are structural system properties that may show acceptable small variations depending of the sensor locations, however, the mode vectors do depend on the sensor locations and they require considerable engineering expertise. Numbers of the locations was decided for spatial resolution to distinguish the close modes or weakly appeared modes and construct the mode shapes in accordance with those of the true finite element model. The most likely reasons behind indistinguishabilty are; (1) it is physically possible that the sensor points are less relevant in modes or (2) excitation is insufficient to trigger some modes out of the active modes in a frequency band of interest or (3) the measurement is not sufficiently long. Every measurement is evaluated whether or not the test structure is nominally linear, weakly nonlinear or strongly nonlinear. The distinction between these categories is somewhat open to interpretation and on how the results are to be used. Deviation from linear behavior may be essential information and the type of nonlinearity may be important for further analysis. Linear behavior is uniquely defined but nonlinear behavior is not, therefore the definition of weak or strong nonlinearity is nonunique (Beyen 2008). In this study, it is proposed that during ambient measurements, structure is statically stable, but in the forced vibration test, due to light damage in some structural members, weak nonlinearity would have been triggered and some differences might be attributed to these damaged members especially in high frequency region.

4 OPERATIONAL MODAL ANALYSIS

4.1 Noise generation and assessment

White Gaussian Noise (WGN) relies on having a good uniform random number generator, which returns a random variable in the range of zero and one. Central limit theory states that the sum of N random number will approach normal distribution as N approaches infinity. As the variance of the generated noise comes close to one with zero mean, signals will have normal distribution. Once we can generate noise signals with normal distribution, we can adjust the signal's mean and variance to use it for any purpose. Therefore, adjustment is open to question and might be discussed. Recorded signals holding structural information are qualified by statistical measures. Following techniques tackle the adjustments on purpose. (1) Signal-to-noise ratio (SNR) is one of the important measures, which is equal to the mean divided by the standard deviation. Better data means a higher value for the SNR. To suite the Gaussian noise input with a specified SNR to real noise source in present physical condition is hard task if there is no any such information a priori. (2) Alternatively, generating white Gaussian noise with a specified power which, has a physical meaning might be preferred if the power is approximated depending upon the size of the problem. (3) As an option to 2, power information might be collected from received output data after filtering structural effects within the structural frequency interest. Techniques used to generate WGN in OMA are studied for the real ambient and forced vibration data.

4.1.1 Type 1: Artificial input noise which, is based on stochastic numbering estimation, is generated using some value like 15 (representing dirty white noise, i.e., coefficient of variance is around 7%) for both ambient and forced vibration test data. Generated noise history and power spectral density are plotted in Figure 5. In Figure 6, transfer functions (smoothed by Hamming window) for the ambient and forced responses are calculated between the structural points and the input noise (type-1) for x and y directions.

4.1.2 Type 2: WGN whose power is equal to the power of the structural response recorded at the first floor is preferred this time. Critical issue here is to select the floor, which is participated in the responses with very small interaction (i.e., mass-participation-factor or displacements of the modes small and approaching to zero). For both ambient and forced test data, calculated and estimated values of the power density of the synthetic input are given in table 4. Consistencies between the values of the power spectral density for recorded and generated signals are observed. Transfer functions in cases of ambient and forced vibrations are plotted in Figure 7.

4.1.3 Type 3: As an option to type 2, this time, WGN input is simulated based on power of the response history after high pass filtering the data beyond the structural frequency interest (i.e., deciding filter corner frequency from power spectra or spectral density plot). Filtering out the influence of the structure remains relatively less affected natural signals. Therefore, it is believed that the power of the filtered signal might be accepted as a threshold value for the source model, which is more representative for the real physical conditions. In Figure 8, this scheme was applied for both ambient and forced test data using the WGN input with the power estimated as explained.

Transfer functions for ambient and forced vibration cases are when compared with the transfer functions (i.e., target ones) estimated from real input output couples. Followings are seen worthy to point out;

(a) Adapting OMA in case of force vibration yields almost similar shapes of the transfer functions, peak frequencies, as well as frequency bands (i.e., broadband structure). Coupled peaks are also identified very closely; therefore, envelopes of the transfer functions look similar with the exceptions of peak values. When the transfer functions with all types of WGN inputs in Figures 6, 7 and 8 are compared with the target one in Figure 4. Type-1 (with S2N ratio) producing largest maxima in all cases needs to be precisely estimated especially for forced vibration studies. Type 3 (identical to power of the filtered response history) yields better transfer function estimation for ambient and forced vibration cases.
(b) Results of the generated WGN inputs among the three schemes do not only show inconsistency in peak values of the transfer functions in forced vibrations but also same problem is seen for ambient vibration conditions.
(c) Prediction and/or generation of unmeasured input signal (noise) actually have a scale problem. It is arguable but If a unique WGN input history is utilized for all cases, effect of the differences in peaks may become ignorable.

4.2 Operational Modal Analysis in the Presence of Harmonics

In OMA, measured operational responses of a system are used to estimate the modal properties of the structure. Due to unmeasured input motion, for instance, masses participated in modes cannot be estimated truly; therefore mode shapes are not scaled beside incorrect modal damping ratios. In case of the forced vibrations, filtering out the harmonic responses or discriminating the poles of the forced response peaks might be remedy under certain conditions (i.e., inputs at Eigen frequencies) for a practitioner who uses the results carefully for further procedure. However, they and some other similar techniques are not advisable for many people in practice. As an easy way, working with stories' spectra in OMA, with unmeasured input motion, supplies characteristic and true operational response information. Estimation of the transfer functions in-between the floors (i.e., rigid diaphragms in civil engineering structures) in ascending order starting from first to roof level is easy and robust technique. Transfer functions might be either in time or frequency domain estimated from harmonic responses of the stories. In calculation, responses of the stories cancel out inherently exist harmonics of each other. To demonstrate the idea for real field case, relative story transfer functions are estimated and plotted in Figure 9 for one of series of instruments located at the corner-1 for one of the forced vibration cases as an example. WGN is used as the input data for the first floor in order to be understood the entire behavior in-between the stories. As seen from the figure 9, Due to weak WGN inputs, spikes in some story transfer functions are appeared in ambient condition, in contrast to this fact, in forced vibrations due to nonlinearity (i.e., damaged members whose damping is participated) such spikes are eliminated, however similar peaks at similar frequencies are observed with smaller amplitudes. Increasing number of peaks in a story in high frequency region might be sign of damage or possible progressive damage (Law et al. 1993). In general, sound consistency in peak frequencies as well as amplitudes after 3 Hz is observed. It is expected that the technique will work for the structure with no damage for both cases.

4 CONCLUSIONS

In this study, assessment of the input noise, power of the input and influence to results is studied using real test data recorded from insitue experiments. Transfer functions inferred from ambient and forced vibration data are compared with the target transfer functions of the real input output couples. Results of the generated WGN inputs among the three schemes show consistent peak frequencies, shapes and very close transfer function envelopes. However, variations in peak values in forced vibrations and in ambient vibration conditions show that prediction and/or generation of unmeasured input signal (noise) actually have a scale problem. It is arguable but If a unique WGN input history is utilized for the structure in all cases, effect of the differences in peaks may become ignorable. Estimation of the transfer functions in-between the floors in ascending order starting from first to the roof level in time or in frequency domain cancels out harmonic response of each story. Results are promoting the application possibilities for undamaged structures for ambient and forced vibration conditions.

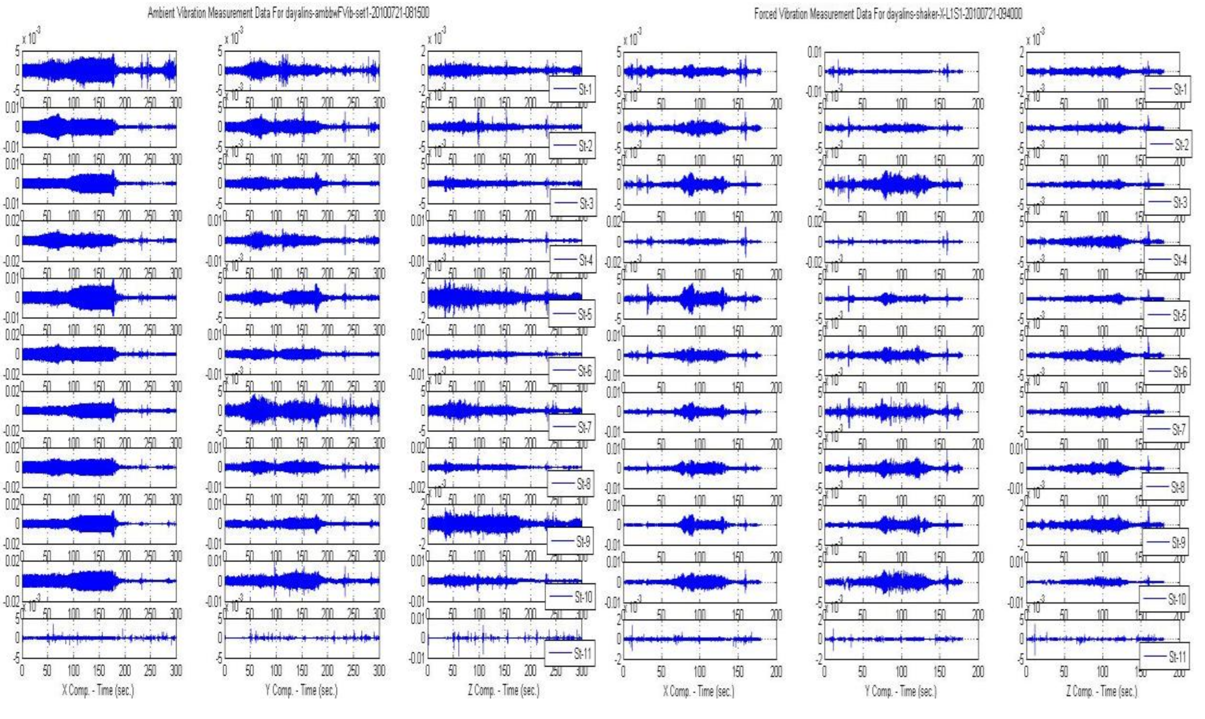

Figure 2 : First 3 columns in the left, ambient vibration time histories recorded on Dayalins with 10 three component accelerometers located on structural observation points and microtremor time histories at station 11 at the free field. Last 3 columns for harmonic excitation.

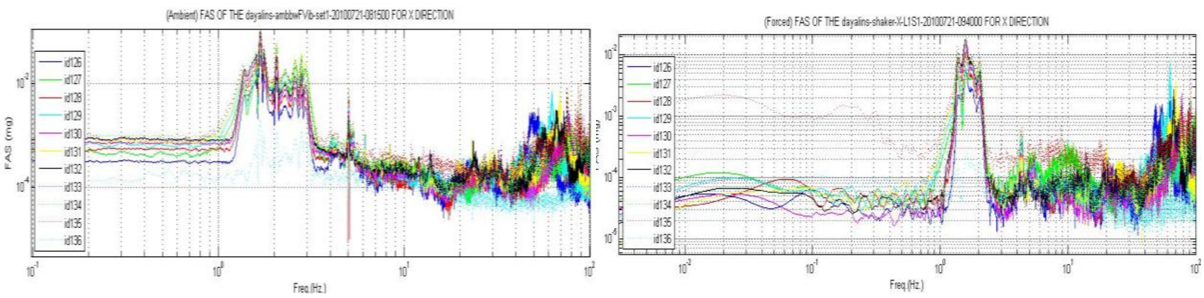

Figure 3 : Fourier Amplitude spectra of the Ambient data recorded on Dayalins bare frame structure and microtremor time history at the free field, left. FAS of the Forced vibration on the right.

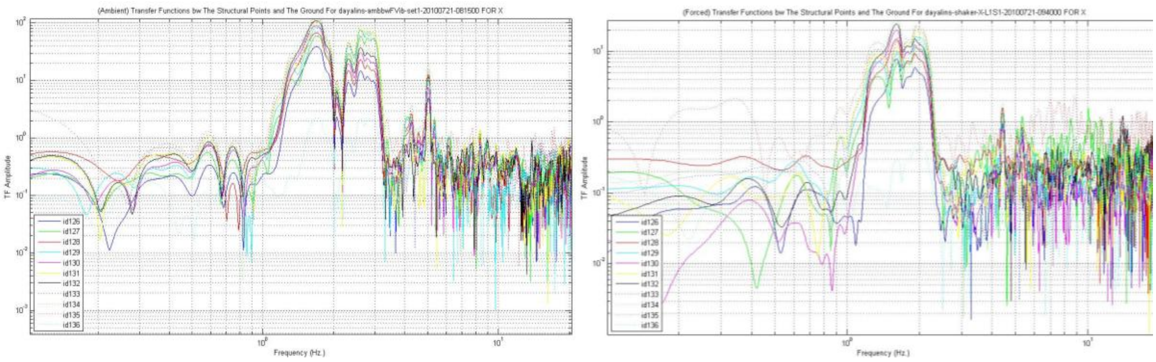

Figure 4 : Structural transfer functions for ambient vibrations with respect to free field data for x direction (left), in case of forced vibration in the right.

Table 1 : Modal Frequencies and Damping Ratios for Forced Vibration in x Direction

	mode 1	**mode 2**	**mode 3**	**mode 4**	**mode 5**	**mode 6**	**mode 7**	**mode 8**	**mode 9**	**mode 10**	**mode 11**	**mode 12**
Modal Freq. (Hz.)	1,429	1,662	1,916	2,013	4,348	5,397	7,536	14,000	17,482	24,983	47,668	48,695
Modal damp. Ratio	2,445	5,234	11,958	33,145	3,199	4,891	8,343	2,699	7,030	2,374	1,574	1,376

Table 2 : Modal Frequencies and Damping Ratios for Ambient Vibration in x Direction

	Mode 1	**Mode 2**	**Mode 3**	**Mode 4**	**Mode 5**	**Mode 6**	**Mode 7**	**Mode 8**	**Mode 9**	**Mode 10**	**Mode 11**	**Mode 12**
Modal Freq. (Hz.)	1,442	1,707	2,284	2,794	5,065	7,956	12,238	13,912	27,298	30,555	48,590	50,002
Modal damp. Ratio	4,330	2,144	29,985	4,082	0,684	5,004	5,580	2,149	2,007	1,848	1,714	2,073

Table 3a : Modal Displacements For The First Twelve Modes For Ambient Vibration in x Direction

Modal Displacements of the Identified Modes in x for the Ambient Data of Dayalins													
St.no	**Inst.no**	**mode1**	**mode2**	**Mode3**	**mode4**	**mode5**	**mode6**	**mode7**	**mode8**	**mode9**	**mode10**	**mode11**	**mode12**
St1	**id126**	0,267	0,287	0,201	0,156	0,555	0,667	0,398	0,263	0,128	0,079	1,000	1,000
St2	**id127**	-0,047	0,458	0,484	0,727	0,583	-0,428	-0,221	0,237	0,126	-0,141	-0,050	-0,027
St3	**id128**	0,489	0,494	0,315	0,246	0,624	0,256	-0,604	-0,568	0,175	-0,219	-0,028	-0,033
St4	**id129**	-0,076	0,657	0,686	0,954	0,481	0,221	0,328	-0,804	0,191	-0,483	0,155	-0,041
St5	**id130**	0,674	0,660	0,389	0,328	0,364	-0,494	-0,490	-0,169	-0,216	-0,298	-0,016	0,042
St6	**id131**	-0,101	0,807	0,823	1,000	0,140	0,667	-0,046	-0,221	-0,249	-1,000	0,055	-0,011
St7	**id132**	0,821	0,805	0,463	0,409	-0,246	-0,553	0,601	0,915	-0,546	-0,740	-0,037	-0,128
St8	**id133**	-0,117	0,905	0,898	0,858	-0,310	0,302	-0,585	1,000	-0,481	-0,842	0,012	0,131
St9	**id134**	1,000	0,931	0,478	0,470	-1,000	0,375	-0,397	-0,688	-1,000	0,494	-0,079	0,103
St10	**id135**	-0,146	1,000	1,000	0,563	-0,788	-1,000	1,000	-0,748	-0,949	0,639	0,073	-0,115

Table 3b : Modal Displacements For The First Twelve Modes For Forced Vibration in x Direction

Modal Displacements of the Identified Modes in x For the Forced Vibration Data of Dayalins													
St.no	**Inst.no**	**Mode1**	**Mode2**	**Mode3**	**Mode4**	**Mode5**	**Mode6**	**Mode7**	**Mode8**	**Mode9**	**Mode10**	**Mode11**	**Mode12**
St1	**id126**	0,219	0,284	0,238	0,505	0,463	0,539	0,429	0,055	0,088	0,618	1,000	1,000
St2	**id127**	-0,178	0,378	0,479	0,435	-0,635	0,818	-0,207	0,169	-0,047	0,225	-0,081	0,027
St3	**id128**	0,485	0,521	0,375	0,380	0,730	0,627	-0,152	-0,538	0,034	-1,000	0,054	0,023
St4	**id129**	-0,305	0,546	0,690	0,644	-0,655	0,669	0,136	-0,725	-0,081	-0,599	0,018	-0,256
St5	**id130**	0,672	0,703	0,493	0,357	0,484	0,371	-0,482	-0,158	-0,011	0,362	-0,036	-0,024
St6	**id131**	-0,395	0,678	0,844	0,760	-0,333	0,247	0,373	-0,046	-0,082	0,314	-0,056	-0,078
St7	**id132**	0,812	0,858	0,606	0,545	-0,106	-0,270	-0,282	0,955	-0,068	-0,440	-0,068	-0,042
St8	**id133**	-0,461	0,773	0,923	0,810	0,247	-0,361	0,143	1,000	-0,132	-0,309	-0,352	0,322
St9	**id134**	1,000	1,000	0,678	0,428	-0,944	-1,000	0,452	-0,791	0,020	0,219	0,199	-0,139
St10	**id135**	-0,574	0,878	1,000	1,000	1,000	-0,967	-1,000	-0,727	-1,000	0,209	-0,039	0,084

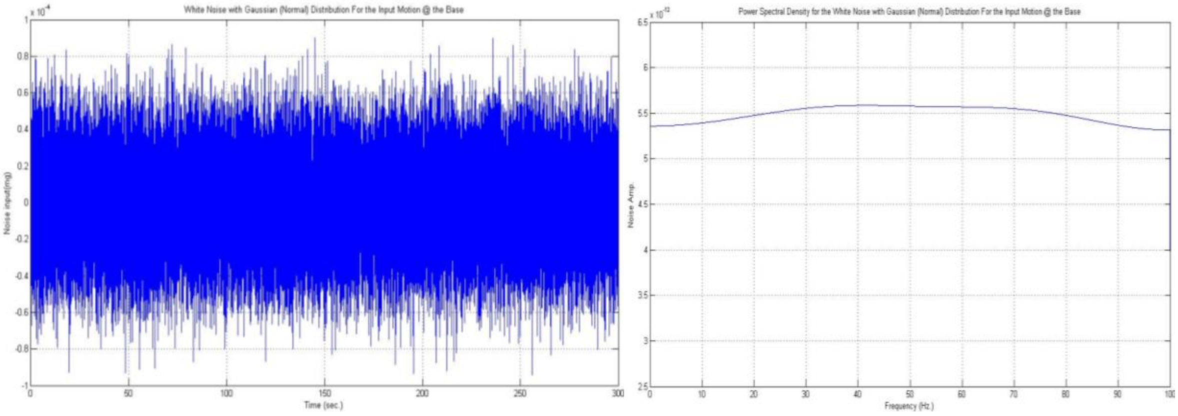

Figure 5 : WGN (type-1) with almost flat power spectral density within the structural frequency interest used as an input data for the ambient output data for x and y directions.

Table 4 : Power Properties of the Recorded and Generated Signals

White Gaussian Noise Generation Based on Power Property			
Data	**Power in Freq Domain**	**Power in Time Domain**	**Average Power**
Recording_X	1,87E-06	1,13E-06	-5,73E+01
Recording_Y	3,76E-07	3,02E-07	-6,42E+01
white Gaussian Noise_X	1,85E-06	1,85E-06	-5,73E+01
white Gaussian Noise_Y	3,73E-07	3,78E-07	-6,42E+01
Filtered Recording_X	9,95E-04	1,23E-03	-7,00E+01
Filtered Recording_Y	2,46E-03	1,96E-03	-6,61E+01
WGN_Xf	9,99E-04	1,00E-03	-7,00E+01
WGN_Yf	2,45E-03	2,44E-03	-6,61E+01

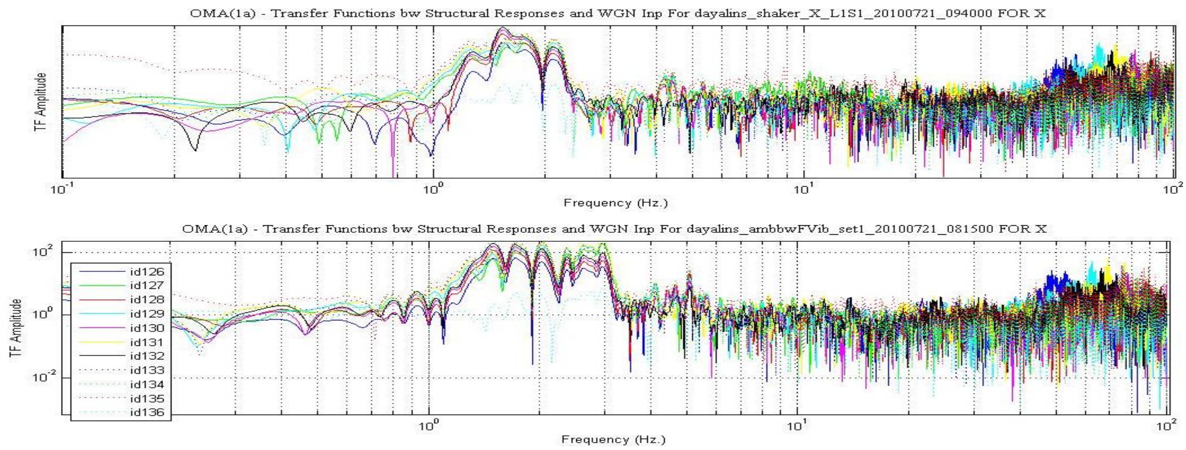

Figure 6 : Transfer functions for ambient and forced vibration data, between the structural points and the white Gaussian noise input data (type-1) are estimated for x and y directions. TFs are from top to down respectively for forced and ambient vibration cases.

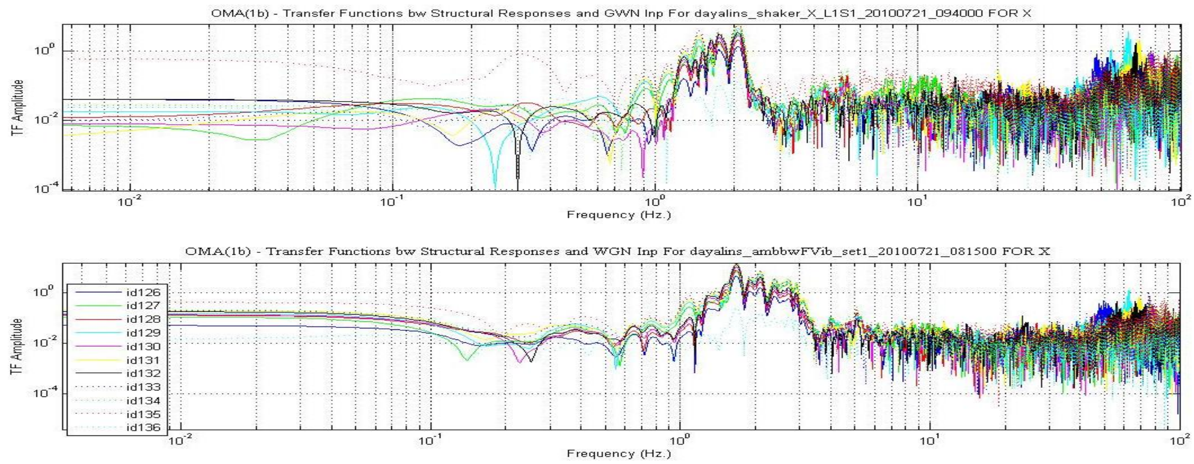

Figure 7 : Transfer functions for ambient and forced vibration data, between the structural points and the white Gaussian noise input data (type-2) are estimated for x and y directions. TFs are from top to down respectively for forced and ambient vibration cases.

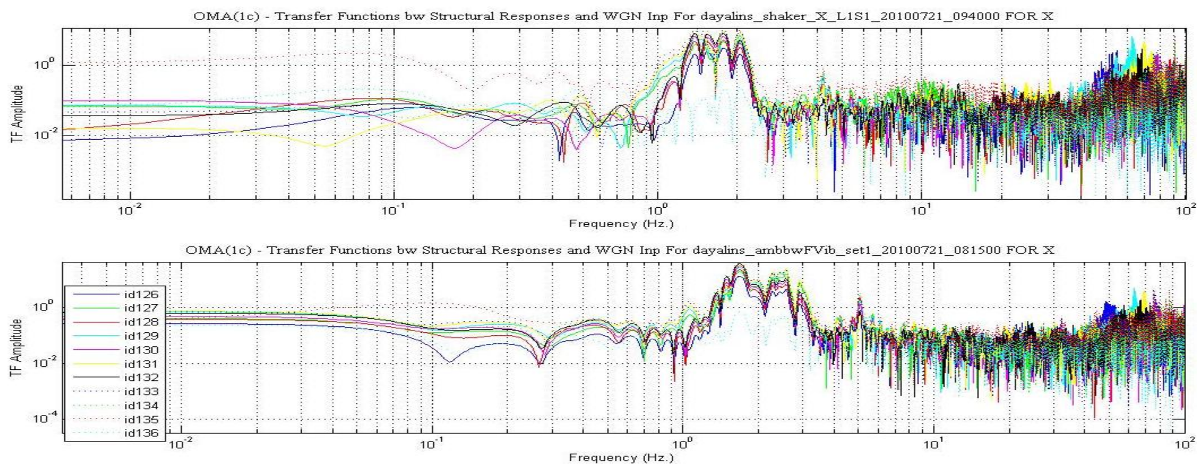

Figure 8 : Transfer functions for ambient and forced vibration data, between the structural points and the white Gaussian noise input data (type-3) are estimated for x and y directions. TFs are from top to down respectively for forced and ambient vibration cases.

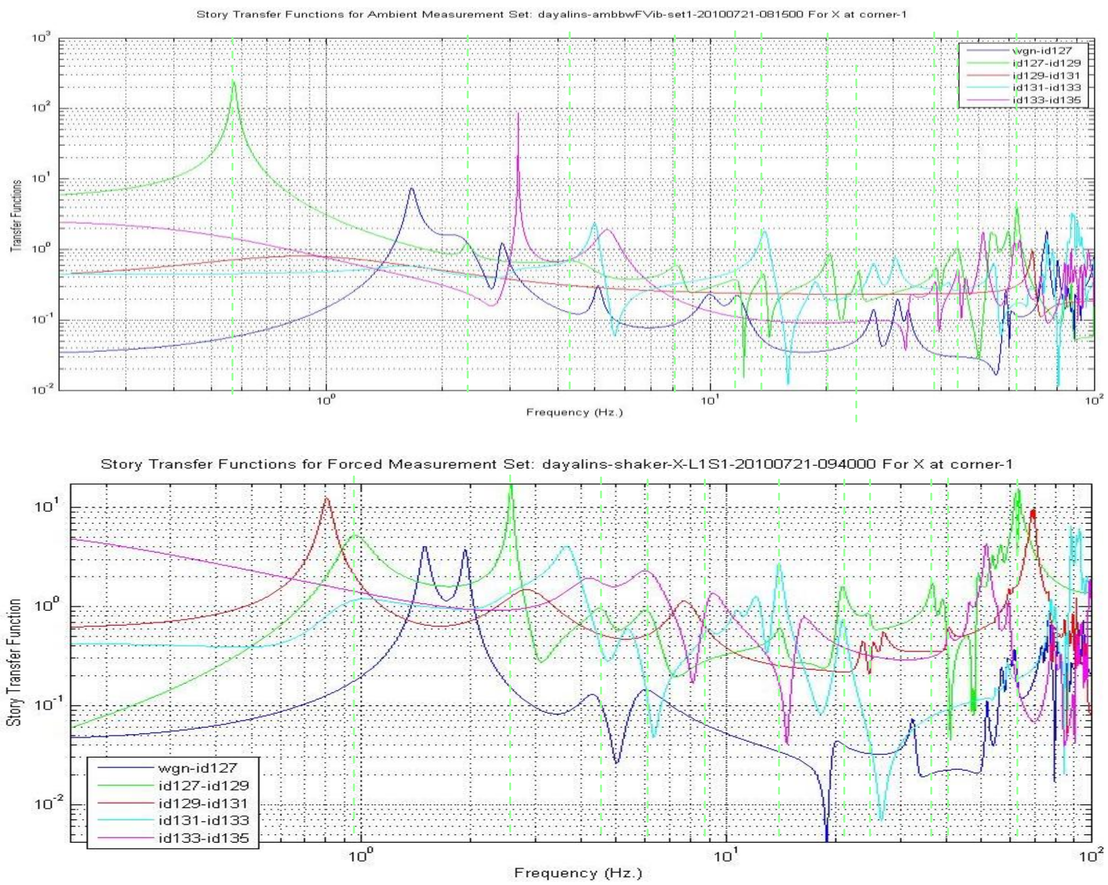

Figure 9 Story transfer functions of the structural observation points (at corner-1) for ambient (top) and forced (below) vibration data for x between the floors from base to top floor. White Gaussian noise is used as the input data for the first floor in x direction.

ACKNOWLEDGEMENTS

A part of the research work has been conducted in the framework of the TUBİTAK research project No. 108M303. The support of the TUBİTAK is gratefully acknowledged.

REFERENCES

Juang, J.-N., 1994, *Applied System Identification*, Prentice Hall, Englewood Cliffs, New Jersey, 07632.

Juang, J.-N., Pappa, R. S., 1985, An Eigensystem Realization Algorithm for Modal Parameter Identification and Model Reduction, *Journal of Guidance, Control, and Dynamics*, Vol. 8, No.5.

Law, S. and Li, X., 1993, Structural damage detection based on higher order analysis, *Procedings of Asia Pacific Vibration Conference*, Japan, 640/3.

Mathworks, 2002, *Signal Processing Toolbox for Matlab*, Ver. 6.5, The MathWorks Inc., Natick, MA.

Arel deprem İzleme Sistemleri, 2010, AREL-DAC serisi, http://www.areldeprem.com.tr

Beyen, 2008. Structural Identification for Post-earthquake safety analysis of the Fatih mosque after the 17 August 1999 Kocaeli earthquake, *Engineering Structures*, Volume 30, Issue 8, pages, 2165-2184.